

1 **Optimization of MQWs for PL Emission and investigation of highly**
2 **reflective p-electrode (Ni/Mg) as well as p-AlGaN contact surface**
3 **condition for the design of UV-B LEDs.**

4 M. Ajmal Khan^{1*}, Noritoshi Maeda,¹ Masafumi Jo,¹ Yuki
5 Akamatsu,³ Ryohei Tanabe,³ Yoichi Yamada,³ and Hideki Hirayama¹

6 Before making the actual 310nm-and 295nm-UVB LEDs devices we attempted for
7 several type of optimization conditions to engineer the bandgap of n-AlGaN buffer layer,
8 current spreading layer and ultimately the active region (MQW) grown on AlN template for
9 the desired emission wavelength. When we used the growth time about 12 sec for the QWs
10 (2nm-4nm) and 24 sec for the QW barrier (8-10nm) of the 3-fold MQWs then the PL
11 emission intensity from the AlGaN MQWs in the range 300nm-315nm increased
12 significantly. When we used the growth time about 15 sec for the QWs (2 nm-3 nm) and 34
13 sec for the QW barrier layers (6-7nm) of the 3-fold MQWs then the PL emission intensity
14 from the AlGaN MQWs in the range 280nm-300nm increased significantly. Subsequently,
15 IQEs around 40 or 50% were confirmed for both 310nm-band and 295nm-band UVB
16 emission respectively with single peak photoluminescence from MQWs grown on low TDDs
17 AlGaN graded layer. The structure consist of two-fold AlGa_{0.65}N(2-3nm)/Al_{0.48}Ga_{0.52}N(6-
18 8nm) MQWs for EL emission wavelength at 294nm or three-fold
19 Al_{0.44}Ga_{0.56}N(4nm)/Al_{0.5}Ga_{0.5}N (20nm) MQWs for EL emission wavelength at 310 nm.

20 Figure I (a) shows (0002) ω -2 θ scan for MQWs grown on n-AlGaN and graded buffer
21 layers on an AlN template (XRCs of the n-AlGaN current spreading layer and the graded
22 AlGaN along (0002) zone axis are shown in the inset of Fig. I(a)). It shows the XRC of the
23 first n-AlGaN layer on AlN (red color) and the final n-AlGaN layer on the graded AlGaN
24 layer (green color), which have FWHMs of 474 and 591 arcsec for (0002) diffraction,
25 respectively. Figure I (b) shows the PL emissions spectra of both AlGaN buffer layer and
26 AlGaN-MQW on the overlayer together to engineer the emission wavelengths between
27 290nm and 330nm respectively at room temperature (RT), by using a 20mW Ar-SHG (244
28 nm) laser as an excitation source. Fig. I(b), gives single-peak emission for every UVB
29 samples between 290nm to 320nm. The deep-level emissions were two orders of magnitude
30 smaller than that of the main peak of active region (MQWs) grown on the graded AlGaN

1 layer. By quick check 42 % IQE from 310nm-UVB MQWs and 50 % IQE from 295nm-UVB
2 MQWs were estimated respectively at low temperature, (77K) as well as at RT (290K) PL
3 measurement.

4 Before the real implementation of the Ni/Mg p-electrode on the UVB LED devices, we
5 investigated the individual reflectance of each metallic layer as shown in the Figure II(a),
6 where the schematic diagram of the samples were used during the investigation and
7 evaluation of the reflectivity from Ni/Mg, Mg, Ni/Al and Al p-electrodes were also given.
8 The introduction of a very thin Ni layer is quite important to make an electrical contact on p-
9 AlGaN layer for UVB LED range and to avoid unnecessary absorption by Ni layer. The
10 reflectivity of the Ni/Al electrode is heavily dependent on the Ni layer thickness. However,
11 the use of Ni/Al p-type electrodes with thin Ni layers was rather a problem [28-29], because
12 the reliability of the UVC and UVB LEDs grown on AlN template with p-electrode made
13 from Ni/Al are currently under investigation. It is also important to mention here that 70%
14 reflectance from p-electrode is still not sufficient for high LEE in UVB LEDs applications.
15 Therefore we need more than 90% reflectance from the p-electrode in order to obtain high
16 LEE, by taking into account the number of reflections of light that made inside the LED
17 structure. Therefore it is very important to search for a new type of p-electrodes with
18 sufficient high reflectivity in order to obtain high LEEs for UVB LEDs with reasonable
19 reliability and stability conditions.

20 Different p-type electrodes like Ni(20nm)/Au (150nm), Ni(1nm)/Mg(200nm),
21 Mg(200nm), Ni(1nm)/Al(200nm), and Al(200nm) were evaporated on the sapphire
22 substrates by using the conventional vacuum evaporation system used for the LEDs.
23 Subsequently the reflectivity from Ni/Au, Ni/Mg, Mg, Ni/Al and Al p-electrodes were
24 measured by using standard optical measurement system [28,29]. Figures II(a)-II(b) shows
25 the relative reflectance of Ni(1nm)/Mg(200nm), Mg(200nm), Ni(1nm)/Al(200nm), and
26 Ni(30nm)/Au(150nm) layers directly deposited on the c-sapphire substrates and calibrated
27 by the reflectance of an Al/sapphire reference sample. The measured values of the relative
28 reflectivity for UV-B emission around 300nm are approximately 1.03, 0.88, 0.83, and 0.34
29 for the Mg, Ni/Mg, Ni/Al, and Ni/Au electrodes, respectively, as shown in Fig. II(b) and
30 could be higher for the upper bound emission of 315nm, UV-B LED devices. But the actual
31 reflectivity of Ni/Au and Ni/Mg are approximately 30-34% and 80-81% respectively [28].

1 In this work, we implemented the same p-electrode model of Ni/Au and Ni/Mg p-electrodes
2 and analyzed the improvements in the LEE made by replacing the conventional Ni/Au p-type
3 electrodes with highly-reflective (novel) Ni/Mg electrodes in both 310nm- and 295-band
4 UVB LEDs devices respectively. We measured the LEE enhancement factors of these new
5 UVB devices and found that the obtained LEE enhancement factor is around 1.3 time, which
6 were caused by the reflectivity of the Ni/Mg electrodes, as shown in Figs. 5 and 6 of this
7 article. The reason for the high LEE enhancement factor of 1.3 times increase in the
8 reflectivity from approximately 34% (Ni/Au) to 88% (Ni/Mg) as shown in the Fig. II(b).

9 Ni/Mg base p-electrode could be encounter with oxidation issue but there are few ideas
10 about the encapsulation/packaging of the In, n-electrode and Ni/Mg p-electrode in LED
11 devices that the oxidation issue could be catered. Maeda et al., investigated the degradation
12 in the reflectance of the Ni/Mg electrodes by the oxidation of Mg given in the figure 6 of
13 reference [28-29]. Comparison was made between the measurements obtained immediately
14 after evaporation and those obtained after 4 months. It was concluded that the maximum
15 EQE fall from 6.6 to 6.0% after 4 months. We speculate that the thin MgO layer could be a
16 natural encapsulation for the Ni/Mg electrode but we still need to check the life of Ni/Mg p-
17 electrode by testing it after longer time. To avoid oxidation issue some alternative ideas have
18 been discussed, especially passivation layer is required for Ni/Mg electrodes to prevent the
19 degradation of the LED performance by the oxidation of Mg. One another option could be
20 the encapsulation of the Ni/Mg p-electrode immediately just after the device fabrication. Rh
21 were investigated by Maeda et al., for UVC LED and quite promising results were achieved,
22 but it is still under investigation for reproducibility and reliability purposes [28,29], because
23 the growth of Rh p-electrode is difficult in the conventional evaporation system due its high
24 melting point around 1964 °C. As for as the n-electrode is concerned, we used Indium (In)
25 based n-electrode, which is very low resistive, having a suitable work function for n-AlGaIn
26 and can easily be fabricated on the UV-B LED device for quick check. If properly
27 encapsulated or passivated then the oxidation could possibly be avoided. But actually the
28 flip chip, which is made from Ti/Al/Ti/Au is the standard n-electrode for UVC LEDs as
29 given in the references [19,20,28] and flip-chip could possibly enhanced the UVC LED
30 devices performance. We will use flip-chip on UVB LED structure in the future and we can
31 expect some higher EQE from our UVB LED devices. This is our near future plan.

1 Figure III shows the optical microscopy image of the p-AlGa_N contact layers of, (a)
2 310nm-band UVB LED and (b) 295nm-UV-B LED grown in the LP-MOVPE system. The
3 AlGa_N UVB LED synthesis on AlN template on sapphire substrate by LP-MOVPE has
4 many advantages, for example to grow LED device in a short span of time on large-area of
5 wafer. Fig. III(a) shows optical microscopy image of the final p-AlGa_N thin layer of 295nm-
6 band UVB LED which exhibiting very clean surface without residues of heavy metals etc
7 except small cracks as depicted in the small circle. On the other hand such small crack were
8 also found in the excess number on the surface of p-AlGa_N 310nm-band UVB LED, as
9 shown in Fig. III (b). We need to overcome these small crack on the front of p-AlGa_N contact
10 layer prior to the p-electrode evaporation in the near future to improve the electrical
11 conductivity as well as p-contact for EIE.

12
13
14
15
16
17
18
19
20
21
22
23
24
25
26
27
28
29
30
31
32
33

1 **Figure captions**

2

3 **Fig. I** (a) (0002) ω - 2θ scan for MQWs grown on n-AlGaIn current spreading and graded
4 buffer layers including active region on an AlN template (XRCs along (0002) zone axis are
5 shown in the inset), and (b) photoluminescence (PL) spectra of fabricated AlGaIn MQWs
6 grown n-AlGaIn graded buffer layer and peak emission wavelengths between 290nm and
7 330 nm, at room temperature (RT) with excitation power of 20 mW.

8

9 **Fig. II** Schematic diagrams of the test samples of p-electrodes used for evaluating the
10 reflectivity from (a) Ni/Mg, Mg, Ni/Al and Al, layers directly deposited on sapphire wafers
11 (b) relative reflectance of Ni(1nm)/Mg(200nm), Mg(200nm), Ni(1nm)/Al(200nm), and
12 Ni(30nm)/Au(150nm) stacking layers directly deposited on sapphire substrates calibrated by
13 the reflectance of an Al/sapphire reference sample.

14

15 **Fig. III** Optical microscope images of the p-AlGaIn contact layer of (a) 290nm-band UVB
16 LED, and (b) 310nm-band UV-B LED prior to the p-electrode and n-electrode formation.

17

18

19

20

21

22

23

24

25

26

27

28

29

1
2
3
4
5
6
7
8
9
10
11
12
13
14
15
16
17
18
19
20
21
22
23
24
25
26

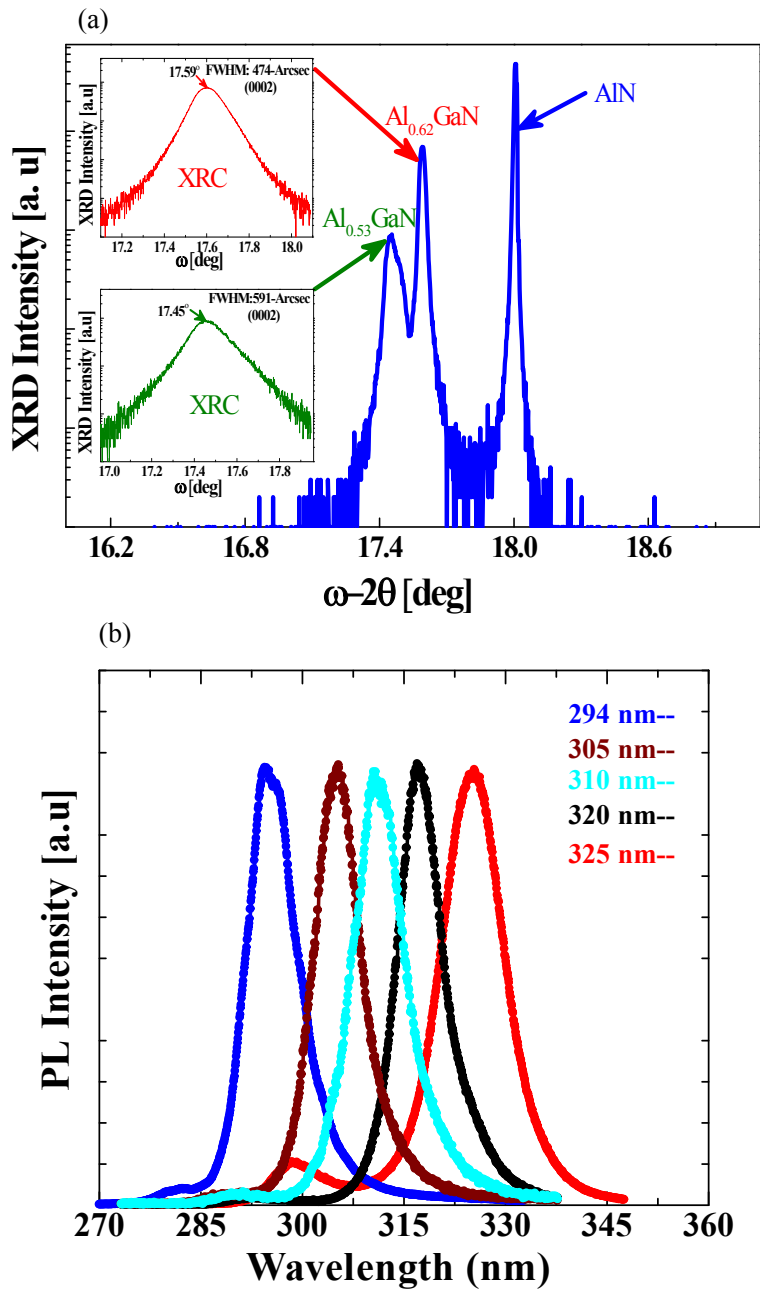


Fig. I Khan et al

1
2
3
4
5
6
7
8
9
10
11
12
13
14
15
16
17
18
19
20
21
22
23
24
25
26

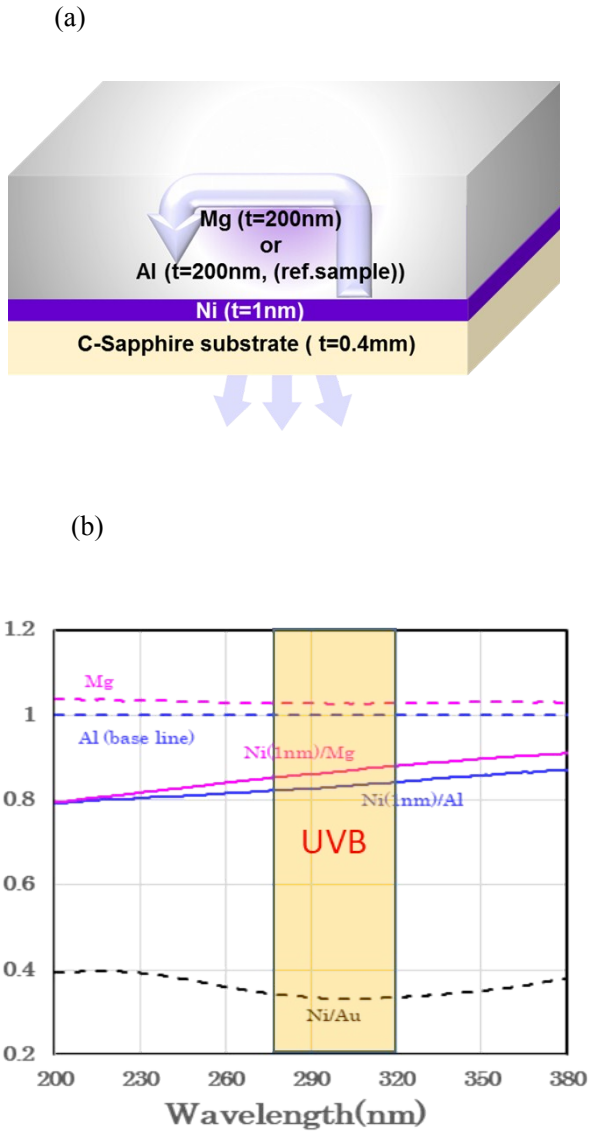


Fig. II Khan et al

1
2
3
4
5
6
7
8
9
10
11
12
13
14
15
16
17
18
19
20
21
22
23
24
25

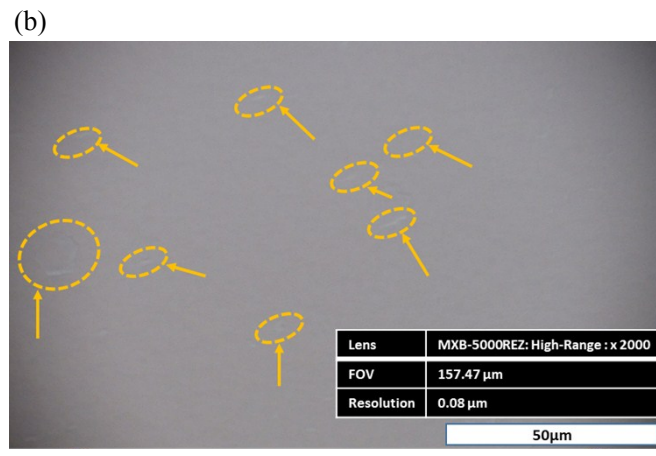
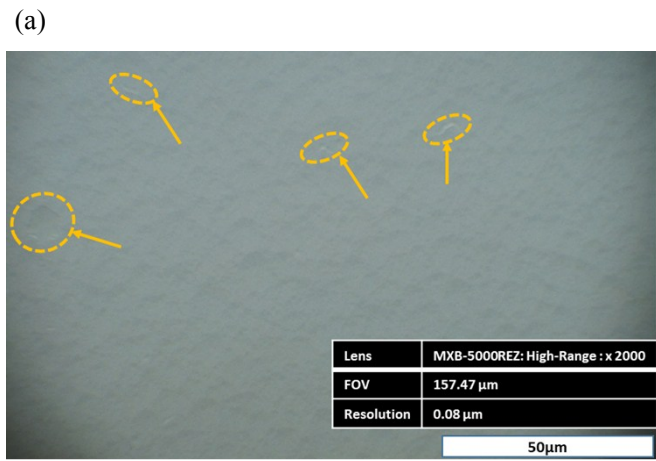


Fig. III Khan et al